ICYM^{2}I: THE ILLUSION OF MULTIMODAL INFORMATIVENESS UNDER MISSINGNESS

Anonymous authors
Paper under double-blind review

ABSTRACT

Multimodal learning is of continued interest in artificial intelligence-based applications, motivated by the potential information gain from combining different types of data. However, modalities observed in the source environment may differ from the modalities observed in the target environment due to multiple factors, including cost, hardware failure, or the perceived *informativeness* of a given modality. This shift in missingness between the source and target environment has not been carefully studied. Naïve estimation of the information gain associated with including an additional modality without accounting for missingness may result in improper estimates of that modality's value in the target environment. We formalize the problem of missingness, demonstrate its ubiquity, and show that the subsequent distribution shift results in bias when the missingness process is not explicitly accounted for. To address this issue, we introduce ICYM^{2}I (In Case You Multimodal Missed It), a framework[1] for the evaluation of predictive performance and information gain under missingness through inverse probability weighting-based correction. We demonstrate the importance of the proposed adjustment to estimate information gain under missingness on synthetic, semi-synthetic, and real-world datasets.

1 INTRODUCTION

Multimodal learning is ubiquitous in machine learning as practitioners combine multiple data types to improve predictive performance in applications to healthcare (Perochon et al., 2023; Tu et al., 2024), robotics (Gao et al., 2024; Shah et al., 2023), and recommender systems (Chen et al., 2019). However, factors such as privacy concerns (Jaiswal & Provost, 2020; Zhang et al., 2021), cost-benefit tradeoffs of data-acquisition (Buck et al., 2010), and user preferences (Kossinets, 2006) imprint multimodal data with missingness. Additionally, even if modality complete data is available or curated at training, data noise (Cohen et al., 2004; Ma et al., 2023) and sensor failures (Inceoglu et al., 2021; 2023) may result in missing modalities in the target environment.

Despite the existence of missingness in real-world settings, current multimodal machine learning methods often assume modalities are fully observed, both in source and target environments. When missingness is considered, the literature has focused on engineering efforts (Le et al., 2025; Wu et al., 2024) such as data selection (Hosseini et al., 2022), imputation (Tran et al., 2017; Cohen Kalafut et al., 2023; Malitesta et al., 2024), and architecture design (Chen et al., 2022; Zeng et al., 2022), which implicitly assume a stable missingness process between source and target environments. When this assumption is violated, the missingness mechanism induces a distribution shift (Zhang et al., 2023; Liu et al., 2023b) that biases the estimated informativeness of a given modality. Missingness is pervasive and impacts a broad range of application domains encountered in the multimodal literature: in breast cancer screening, biopsies are only performed if there are abnormal findings in a mammogram; in autonomous vehicles, LiDAR sensor dropout can occur due to weather and lighting conditions; and in online recommender systems, reviews are only collected after certain consumer behaviors. Across these settings, ignoring the distribution shift between source and target due to missingness when quantifying modality informativeness may conflate missingness with signal, leading to flawed data collection and modeling decisions.

[1] Available on Github https://anonymous.4open.science/r/ICYM2I-BC18/

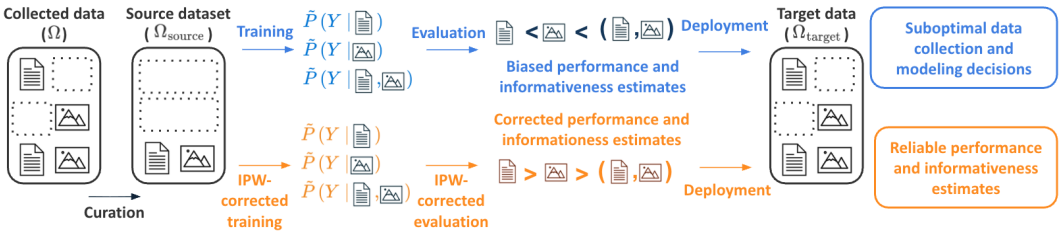

Figure 1. Overview of the proposed framework. Curation often discards missing data, resulting in a discrepancy between the collected Ω and source datasets Ω_{source} used for training. Current practice is denoted in blue: naïve training and evaluating on Ω_{source} leads to biased estimates of performance and informativeness on target data. The orange path illustrates the proposed ICYM^{2}I: a double inverse probability weighting (IPW) mechanism that yields accurate performance and informativeness estimates under the target distribution.

In this work, we propose a framework to overcome the (mis)estimation of both inherent informativeness and predictive utility under missingness in multimodal learning. Our contributions, summarized in Figure 1, are as follows:

- **Framework for multimodal learning with missingness.** We formalize the impact of missingness as a distribution shift *intrinsic* to multimodal learning, where the *observed* source distribution differs from the target distribution due to missingness. We show that not accounting for missingness, a common practice, may bias the estimate of a modality's predictive and information-theoretic utility.
- **ICYM^{2}I.** Under the missingness-at-random (MAR) assumption, a much more realistic assumption than the common and often implicit assumption of missingness-completely-at-random (MCAR) made by state-of-the-art multimodal strategies, we propose ICYM^{2}I (In Case You Multimodal Missed It), a double inverse-propensity weighting correction to overcome missingness-induced distribution shifts. Specifically, we demonstrate that ICYM^{2}I improves correlation in predictive and information-theoretic utility of modalities.
- **Experiments on diverse data.** We demonstrate the broad applicability and utility of our methods in synthetic, semi-synthetic, and real-world benchmark datasets, including a case study in multimodal learning in health.

2 Related Work

Multimodal benchmarks suppress missingness encountered in real-world environments. Prior work on multimodal models often assumes *fully observed modalities* (Ngiam et al., 2011; Zadeh et al., 2017; Hou et al., 2019). Missingness has largely been an overlooked problem (Le et al., 2025; Wu et al., 2024), to the extent that current benchmarks rarely contain samples with missing modalities. Curation often involves dropping incomplete or filtering samples based on data quality criteria, such as text length or file size (Sharma et al., 2018; Schuhmann et al., 2022) or imputing with automatic tools (Miech et al., 2019). This curation implicitly assumes that rejected samples follow the same distribution as the observed ones. This assumption may not hold. For example, in autonomous driving data, samples with sensor failure – often resulting from extreme weather or lighting conditions – may be filtered out. Models trained on complete data may, consequently, not generalize to these settings, creating real-world risk at deployment. When missingness is considered, previous works focused on robustness through imputation (Tran et al., 2017; Cohen Kalafut et al., 2023; Malitesta et al., 2024), representation learning (Wu et al., 2024; Liu et al., 2023a), knowledge distillation (Li et al., 2024; Wang et al., 2020a), and model ensembling (Chen et al., 2022; Zeng et al., 2022) – all ignoring the potential shift resulting from the missingness process.

Multimodal missingness in the target environment. Prior work has explored missingness in the target environment (Lin & Hu, 2023; Zeng et al., 2022), e.g., when a captor fails at deployment (Ma et al., 2022). Broadly, two strategies have been proposed (Wu et al., 2024): (i) data preprocessing through cross-modal imputation (Cohen Kalafut et al., 2023; Malitesta et al., 2024; Tran et al., 2017), where one replaces the missing modality (Ma et al., 2021; Zhou et al., 2022), as well as (ii) model training strategies such as architecture design (Lee et al., 2023; Ge et al., 2023), distillation-based methods (Li et al., 2024; Wang et al., 2020a), and ensembling (Chen et al., 2022; Zeng et al., 2022). Through the proposed formalization, our work distinguishes between different missingness

assumptions, demonstrating that the previously studied framework is only one among various plausible mechanisms for which current strategies are not well-designed.

Distribution shifts in multimodal learning. Addressing multimodal shifts has been studied in vision-language models (Zhou et al., 2024; Verma et al., 2024) or using information-theoretic notions to understand multimodal behavior under distribution shifts (Oh et al., 2025). Augmentation and regularization strategies have been leveraged to address temporal shifts for conversation understanding (Woo et al., 2023; Lian et al., 2023). Advances in learning, such as in-context learning, have been studied to characterize adaptation to multimodal distribution shifts (Zhou et al., 2024; Xue et al., 2024). However, existing strategies aim to improve robustness under domain distribution shifts, while ignoring the potential shift in missingness between source and target environments.

Quantifying information-theoretic value of a modality. Existing works often implicitly assume that additional modalities improve performance, ignoring the prohibitive cost, complexity, and potential noise added by these additional dimensions. When limited resources or constraints limit availability in the target environment, a central challenge is to quantify the information-theoretic value of a modality (Liang et al., 2024c). Liang et al. (2024a) proposed a method for recovering partial information decomposition measures of the redundancy, uniqueness, and synergy of the information provided by the different modalities (Bertschinger et al., 2014; Williams & Beer, 2010). However, these decompositions fully ignore the impact of missingness.

Correcting for missingness bias. The lack of formalization of missingness in the multimodal literature has led to neglecting its potential impact. Ignoring this process risks biasing estimates of interest (Phelan et al., 2017) as the observed distribution differs from the underlying one practitioners aim to model. The statistical literature has introduced strategies such as matching (Stuart, 2010) and reweighting (Jethani et al., 2022) to correct for the missingness process. However, these works have overlooked the multimodal setting and the systematic shifts that may occur in this setting.

3 Multimodality and Missingness

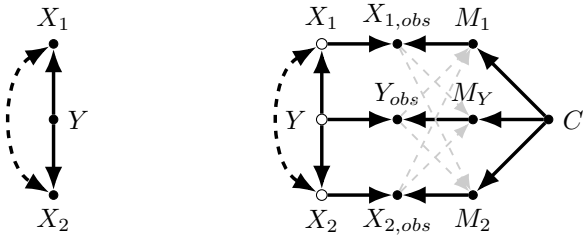

Figure 2. Directed Acyclic Graphs of the assumed data-generating processes. On the left is the commonly assumed graph with no missingness. On the right is the proposed missingness formalism. X_1 and X_2 are two modalities of interest, Y is the label of interest. The missingness process depends on C. Filled point nodes are observed variables, while unfilled nodes are unobserved. Gray edges indicate MAR missingness for a given modality.

Consider two modalities, $X_1 \in \mathcal{X}_1$ and $X_2 \in \mathcal{X}_2$ and the state of interest $Y \in \mathcal{Y}$. We denote the joint underlying distribution $\Omega = \mathcal{X}_1 \times \mathcal{X}_2 \times \mathcal{Y}$. Without loss of generality, we assume an anti-causal setting for the data-generating process, in which the modalities are dependent on the states Y, as shown in Figure 2 (left). We use the binary indicators of missingness M_1, M_2, and M_Y, which are equal to 1 if the associated variable is missing, 0 if observed, following the convention of Mohan & Pearl (2021). Observed variables are subscripted by 'obs', which corresponds to the underlying modality if observed, and unobserved otherwise (denoted by $\varnothing$). Formally, the observed variable Y_{obs} and observed modalities $X_{1,obs}$ and $X_{2,obs}$ can be defined as follows:

$$Y_{obs} = \begin{cases} \varnothing & \text{if } M_Y = 1, \\ Y & \text{otherwise.} \end{cases}$$

In this setting, we denote the observed joint distribution $\Omega_{\text{obs}} := (M_1 \cdot \mathcal{X}_1) \times (M_2 \cdot \mathcal{X}_2) \times (M_Y \cdot \mathcal{Y})$, which has been the focus of multimodal learning. Note that the underlying relation between the covariates of interest X_1, X_2, and Y remains unchanged under the true data-generating mechanism; only the realizations of the observed variables differ.

Missingness in multimodal learning. We distinguish three mechanisms that cover potential missingness in multimodal data (Rubin, 1976):

- Missing Completely At Random (MCAR): A modality is missing completely at random if the missingness process is independent of any other variable.
- Missing At Random (MAR): The missingness mechanism depends on observed variables only.
- Missing Not At Random (MNAR): Missingness depends on unobserved variables.

In Figure 2 (right), we describe the missingness mechanisms as dependent on C, a set of covariates that determine the missingness mechanism. Note that C may include one of the modalities of interest, e.g., whether X_2 is observed may depend on the realization of X_1. In general, the set C may differ for each modality depending on the data-generating process.

Missingness-induced distribution shifts. Missingness in a modality X_i and/or the label Y can induce distribution shifts between the source and the target distributions. For example, if a modality is observed in the target environment only if another one meets some criterion, then this distribution may not match the source distribution. Theoretically, we know that a non-MCAR missingness mechanism induces distribution shifts (Liu et al., 2023b; Zhang et al., 2023), i.e., the observed distribution differs from the underlying distribution. Critically, models trained and evaluated on the observed distribution are statistically biased estimates under any other missingness process.

For instance, consider an autonomous vehicle setting where video and LiDAR represent two modalities of interest. If the LiDAR randomly dysfunctions, the missingness patterns are MCAR. However, as previously mentioned, LiDAR may malfunction under extreme weather conditions. If these conditions can be extracted from the video modality, one may assume MAR patterns. However, if the video cannot capture the variable explaining the LiDAR dysfunction – e.g., temperature – LiDAR would be MNAR, as dependent upon an unobserved variable. Under the last two scenarios, focusing solely on samples with LiDAR excludes all extreme condition settings.

A common and often implicit assumption in the multimodal literature is the absence of missingness, which is analogous to either a MCAR mechanism or a stable missingness process as described in Assumption A. In other words, not adjusting for missingness assumes that the missingness process is uninformative or will remain the same in the target environment.

Assumption A (Stable missingness process)**.** *The missingness process is stable between the source and target environments, i.e., the observed distributions are the same* $\Omega_{obs}^{source} = \Omega_{obs}^{target}$.

A few prior works focus on improving the robustness of multimodal models when performance may degrade due to a modality missing in the target distribution, as formalized in Assumption B.

Assumption B (Collection degradation)**.** *Collection in the target environment may deteriorate, resulting in a distribution shift* $\Omega_{obs}^{source} \sim \Omega \neq \Omega_{obs}^{target}$.

Our work questions the applicability of these assumptions where modality collection is costly. While missingness may naturally present a distributional shift (Zhou et al., 2023), we emphasize that demonstrating the value of a modality in the source environment may lead to increased collection of this modality in the target environment, inducing a distribution shift akin to Assumption C.

Assumption C (Multimodal analysis informs data collection)**.** *Demonstrated multimodal performance gain induces a shift in the missingness process in the target, i.e.* $\Omega_{obs}^{source} \neq \Omega^{target} \sim \Omega$.

We focus on settings where historical data on which one can train a model is marked by missingness. Under such settings, we aim to do the following: (i) identify which modalities are informative and may consequently be fully observed in the target environment, and (ii) train models that generalize to the full observation of these modalities.

4 Is this modality informative?

We aim to assess whether a partially missing modality would be informative if fully observed. To this end, we introduce ICYM^{2}I (In Case You Multimodal Missed It), a framework for correcting model performance trained on modality complete samples where all modalities and labels are observed (Ω_{obs}) to estimate the predictive utility of the partially missing modality if it were observed

for the whole population (Ω). Additionally, we propose a correction to derive unbiased estimates of the information-theoretic utility of a modality, using Ω_{obs}. We rely on Partial Information Decomposition (PID) (Williams & Beer, 2010) bounds introduced by Bertschinger et al. (2014) for this task, which quantifies the information value of a target of interest captured by two input variables.

Correction. We propose an Inverse Probability Weighting (IPW) variant (Robins et al., 1994), which reweights samples based on their probability of being observed. Under Assumption D, IPW recovers unbiased estimates of the true distribution, enabling learning and evaluation on the true distribution from observed samples. IPW-adjustment is critical for both training and evaluation of multimodal models under missingness. IPW-adjusted training results in a model trained to infer on the underlying distribution Ω, while correction of the evaluation allows for measuring performance on Ω, despite evaluating the model only on samples from the observed distribution Ω_{obs}.

Assumption D (MAR and Positivity)**.** *The missingness mechanism is MAR, and* $p_\Omega(M_1 = 0, M_2 = 0, M_Y = 0|C) > 0$.

4.1 A MOTIVATING EXAMPLE

We consider the common multimodal example of learning bit-wise logic operators (Bertschinger et al., 2014; Harder et al., 2013; Liang et al., 2024a). We generate $10,000$ points with two modalities drawn from Bernoulli distributions ($p = 0.5$). The output state Y is defined using the binary operators AND, OR, and XOR of input bits X_1 and X_2. In this setting, we induce missingness M_2 in X_2 and Y as a function of X_1 (MAR): $M_2 \sim Bern(0.6X_1 + 0.2)$, resulting in 50% missingness in X_2. We investigate the impact of missingness on current strategies for evaluating the predictive and information-theoretic utility of a given modality.

Estimating performance for informativeness. A common practice to measure the predictive value of adding a modality is through modality ablation studies where practitioners train models on the subset of observed samples where all modalities are observed (Ω_{obs}). First, unimodal models $f_\phi(x_i)$ are trained to approximate $p_{\Omega_{\text{obs}}}(y \mid x_i), \forall i \in \{1, 2\}$ and a multimodal model $f_\phi(x_1, x_2)$ to approximate $p_{\Omega_{\text{obs}}}(y \mid x_1, x_2)$ on the same observed dataset. The performance is then compared in a hold-out set, which is also sampled from Ω_{obs}. The informativeness of a modality is heuristically attributed to the relative performance gain of the multimodal model compared to the unimodal model. However, multimodal models can perform worse than their unimodal counterparts due to data characteristics (Zhang et al., 2024) and learning dynamics (Wang et al., 2020b; Zhai et al., 2024). Thus, relying solely on performance as a proxy for informativeness, particularly under distribution shifts, can be misleading.

Partial Information Decomposition (Bertschinger et al., 2014). As an alternative to estimating performance, existing works have decomposed the informativeness associated with each modality (Liang et al., 2024a). Partial information decomposition (PID) (Bertschinger et al., 2014; Williams & Beer, 2010) decomposes the total mutual information $I(Y : (X_1, X_2))$ (McGill, 1954; Te Sun, 1980) between a random variable Y and (X_1, X_2) jointly into shared information (information both X_1, X_2 share about Y), unique information 1 (information only X_1 has about Y), unique information 2 (information only X_2 has about Y), and complementary information (information about Y that requires both X_1 and X_2):

$$I(Y : (X_1, X_2)) = \underbrace{SI(Y : X_1; X_2)}_{\text{shared information}} + \underbrace{UI(Y : X_1 \backslash X_2)}_{\text{unique information 1}} + \underbrace{UI(Y : X_2 \backslash X_1)}_{\text{unique information 2}} + \underbrace{CI(Y : X_1; X_2)}_{\text{complementary information}}$$

Let Δ be the space of all distributions over (X_1, X_2, Y) and let Ω denote the true data distribution (without missingness) and define $\Delta_\Omega := \{q \in \Delta : q(X_i = x_i, Y = y) = p_\Omega(X_i = x_i, Y = y)\ \forall x_i \in \mathcal{X}_i, y \in \mathcal{Y}, i \in \{1, 2\}\}$. That is, Δ_Ω is the set of all distributions over (X_1, X_2, Y) such that the two-way joints between X_i and Y match the true data-generating distribution. Equipped with this set, Bertschinger et al. (2014) provides the following bounds $\widetilde{SI}$, $\widetilde{UI}$, and $\widetilde{CI}$ on the analogous quantities:

$$\widetilde{SI}(Y : X_1; X_2) := \max_{Q \in \Delta_\Omega} [I_q(Y : X_1) - I_q(Y : X_1|X_2)] \quad \leq SI(Y : X_1; X_2) \tag{1}$$

$$\widetilde{UI}(Y : X_1 \backslash X_2) := \min_{Q \in \Delta_\Omega} [I_q(Y : (X_1, X_2)) - I_q(Y : X_2)] \geq UI(Y : X_1 \backslash X_2) \tag{2}$$

$$\widetilde{UI}(Y : X_2 \backslash X_1) := \min_{Q \in \Delta_\Omega} [I_q(Y : (X_1, X_2)) - I_q(Y : X_1)] \geq UI(Y : X_1 \backslash X_2) \quad (3)$$

$$\widetilde{CI}(Y : X_1; X_2) := I_\Omega(Y : (X_1, X_2)) - \min_{Q \in \Delta_\Omega} I_q(Y : (X_1, X_2)) \leq CI(Y : X_1; X_2) \quad (4)$$

These bounds are tight if there exists a $q_0 \in \Delta_\Omega$ such that $\widetilde{CI}_{q_0}(Y : X_1; X_2) = 0$. Bertschinger et al. (2014) further shows that under common (but unverifiable) assumptions on the data-generating process, the inequalities are tight for all $q \in \Delta_\Omega$. This results in a compelling argument to rely on these entities, as it suggests that it is not possible to decide whether or not complementary information exists when only marginals (Y, X_1) and (Y, X_2) are known. Hence, we choose this measure of PID. Prior works relying on this PID to attribute information-theoretic value implicitly assume that $\Omega^{\text{source}}_{\text{obs}} = \Omega^{\text{source}} = \Omega^{\text{target}} = \Omega$. Instead, we evidence the limitations of these strategies performed on $\Omega^{\text{source}}_{\text{obs}}$ when the target decomposition is $\Omega^{\text{target}} = \Omega$, i.e., the true data-generating mechanism.

Table 1. Impact of missingness on multimodality information for bitwise logic operators. Parentheses denote standard deviation across batches.

		AUROC			Information Decomposition			
		X_1	X_2	$X_1 + X_2$	Unique 1	Unique 2	Shared	Complementary
AND	Oracle	0.83 (0.01)	0.84 (0.01)	1.00 (0.00)	0.05 (0.00)	0.03 (0.00)	0.26 (0.00)	0.47 (0.00)
	Observed	0.66 (0.01)	0.93 (0.01)	1.00 (0.00)	0.44 (0.00)	0.00 (0.00)	0.15 (0.00)	0.36 (0.00)
	ICYM^{2}I	0.83 (0.01)	0.85 (0.02)	1.00 (0.00)	0.03 (0.00)	0.03 (0.00)	0.27 (0.00)	0.45 (0.00)
OR	Oracle	0.84 (0.01)	0.83 (0.01)	1.00 (0.00)	0.04 (0.00)	0.05 (0.00)	0.27 (0.00)	0.46 (0.00)
	Observed	0.95 (0.01)	0.77 (0.01)	1.00 (0.00)	0.01 (0.00)	0.15 (0.00)	0.10 (0.00)	0.23 (0.00)
	ICYM^{2}I	0.85 (0.02)	0.82 (0.01)	1.00 (0.00)	0.03 (0.00)	0.02 (0.00)	0.27 (0.00)	0.50 (0.00)
XOR	Oracle	0.51 (0.02)	0.49 (0.01)	1.00 (0.00)	0.00 (0.00)	0.00 (0.00)	0.00 (0.00)	0.99 (0.00)
	Observed	0.52 (0.02)	0.80 (0.02)	1.00 (0.00)	0.34 (0.00)	0.07 (0.00)	-0.07 (0.00)	0.62 (0.00)
	ICYM^{2}I	0.53 (0.03)	0.49 (0.03)	1.00 (0.00)	0.00 (0.00)	0.00 (0.00)	0.01 (0.00)	0.96 (0.00)

As a motivating example, we analyze the impact of missingness on estimating PID in the case of unidimensional modalities with a bitwise logic outcome (AND, OR, and XOR). Table 1 (left) presents the discriminative performance associated with neural networks trained on each modality and their combination under three scenarios: (i) access to all data (**Oracle**), (ii) focusing only on datapoints with all covariates observed (**Observed**), and (iii) adequately accounting for missingness (ICYM^{2}I using IPW to adjust $\Omega_{\text{obs}} \mapsto \Omega$, by modeling the missingness mechanism), as proposed in Section 4.2. Table 1 (right) presents PID, discussed in Section 4.3 under the same scenarios, demonstrating how information decomposition is also biased due to missingness.

Specifically, relying on Ω_{obs} overestimates the performance of X_1 for OR but underestimates it for AND. Similarly, biased decomposition results in overestimating the informativeness of X_1 ("Unique 1" compared to "Unique 2") for OR. As X_1 informs the missingness process, it indirectly informs the outcome of interest, despite the true underlying generative process being dependent on both. The use of IPW can correct for such bias under positivity as long as the propensities for IPW can be estimated (i.e., the MAR assumption). We study sensitivity to this assumption in Appendix D, where we further evaluate the robustness of our method under MCAR and MNAR, demonstrating robustness under MCAR.

We now formally describe two methods for reliably inferring the informativeness of modalities using (i) unbiased estimation of unimodal versus multimodal model performance using supervised learning (ICYM^{2}I-learn), and (ii) high-dimensional autodifferentiable partial information decomposition (ICYM^{2}I-PID). In addition, we demonstrate the need for IPW-adjusted *evaluation* as a key element to determine modality informativeness using supervised learning.

4.2 ICYM^{2}I-learn: Estimating performances for informativeness under missingness

Training. Under the MAR assumption, i.e., the missingness is fully explained by observed covariates C; that is, the probability of a data point being missing depends only on C, we propose to train the model with a weighted loss using samples from Ω_{obs}. The proposed IPW-adjusted loss accounts for the distributional shift ($\Omega_{\text{obs}} \mapsto \Omega$) by up-weighting under-observed points, as described in the following lemma.

Lemma 1 (IPW Training). *The loss function computed on the observed data $l_{\Omega_{obs}}(x_1, x_2, y)$ can be reweighted to approximate the target loss $l_{\Omega}(x_1, x_2, y)$ as follows:*

$$l_{\Omega}(x_1, x_2, y) = \frac{1}{1 - p(m_1, m_2, m_y \mid C)} \, l_{\Omega_{obs}}(x_1, x_2, y)$$

where $p(m_1, m_2, m_y \mid C)$ is the probability of missingness, given the covariates C.

Evaluation. Current works suffer from an analogous bias in model evaluation, by relying on a hold-out set from the observed distribution (Ω_{obs}). To estimate a given metric on the true underlying distribution, one must correct this metric using a similar correction as previously described. Li et al. describes how to correct for both AUC and Brier score using IPW.

Corollary 1 (ICYM^{2}I-learn). *Consider a model f trained and evaluated on data drawn from Ω_{obs}. To correct the model and estimate its performance on Ω, one must correct* both *its training and evaluation following the previous corrections.*

4.3 ICYM^{2}I-PID: Partial information decomposition for multimodal informativeness

Under missingness, we have samples from Ω_{obs} instead of Ω. Estimating PID measures in this setting requires adjusting for the $\Omega_{\text{obs}} \mapsto \Omega$ shift. The three-way mutual information is the key estimand of interest to obtain any PID bound, requiring the following correction (derived in Appendix A):

Lemma 2 (Corrected mutual information).

$$I_{\Omega}(Y : (X_1, X_2)) = \mathbb{E}_{\substack{x_1, x_2 \sim p_{\Omega_{obs}}(x_1, x_2) \\ y \sim p_{\Omega}(y \mid x_1, x_2)}} \left[\frac{1 - p(m_1, m_2)}{1 - p(m_1, m_2 \mid x_1, x_2, y)} \log \left(\frac{p_{\Omega}(x_1, x_2, y)}{p_{\Omega}(x_1, x_2) p_{\Omega}(y)} \right) \right]$$

and analogously for other quantities. Second, these mutual information-based quantities can be equivalently estimated using entropy-based measures (see derivations in Appendix B). Third, to enable PID for high-dimensional data, we parameterize q via unimodal neural networks f_1 and f_2, motivated by Liang et al. (2024a). Then,

$$\Delta_{\Omega} \approx \{q \propto \exp(f_1(x_1) \cdot f_2(x_2)) : q(x_i, y) = p_{\Omega_{\phi}}(x_i, y) \, \forall x_i \in \mathcal{X}_i, y \in \mathcal{Y}, i \in \{1, 2\}\}$$

in which Ω_{ϕ} is a re-parametrization of Ω using neural networks and learned using samples from Ω_{obs}. That is, prior work considers $p_{\Omega_{\phi}}(y, x_i) \approx f_{\phi}(y \mid x_i) p_{\Omega_{\text{obs}}}(x_i), \forall i \in \{1, 2\}$, with f_{ϕ}, a unimodal neural network, trained on samples from Ω_{obs} to predict Y.

Due to missingness, $\Omega_{\phi} \neq \Omega_{\text{obs},\phi}$, and should be approximated using IPW corrections for the $\Omega_{\phi} \mapsto \Omega_{\text{obs},\phi}$. We use the modified Sinkhorn-Knopp algorithm (Knight, 2008) to enforce matching the two-way *IPW-corrected* marginals to constraint $q \in \Delta_{\Omega}^{\text{ICYM}^2\text{I}}$[2]. Using the fact that all PID bounds can be obtained by minimizing the three-way mutual information (see Bertschinger et al. (2014), Lemma 4), we summarize our algorithm to minimize $I_q(Y : (X_1, X_2))$ in Appendix C.

5 Experiments

To better understand the connection between performance, information decomposition and missingness, we propose a simulation (detailed in Appendix E), two semi-synthetic studies that reflect real-world missingness mechanisms (see Appendix F), and a real-world case-study.

5.1 Simulation and semi-synthetic experiments

In Table 2, each point represents the estimated PID value (Unique 1, Unique 2, Shared, and Complementary) for one simulation under the training and evaluation IPW-corrections and the oracle performance, i.e., a model trained and tested on Ω. Specifically, columns reflect evaluation correction, while rows reflect training correction. These results underline the importance of correcting

[2]Prior works match conditionals using samples from Ω_{obs} without correction: $q(y \mid x_i) \approx \Omega_{\text{obs}}(y \mid x_i)$ which may produce biased PID bounds.

both training and evaluation, as proposed in ICYM^{2}I, to best align with the performance one would obtain on Ω, as shown by the smallest Root Mean Squared Error (RMSE) observed when both corrections are applied. This observation shows that the proposed ICYM^{2}I best recovers the true informativeness of each modality, despite relying on Ω_{obs}. Appendix E echoes the same observation when evaluating model performance.

Table 2. Comparison between estimated PID using training and PID corrections, and oracle PID on Ω. ϵ denotes the RMSE between estimated and oracle PIDs.

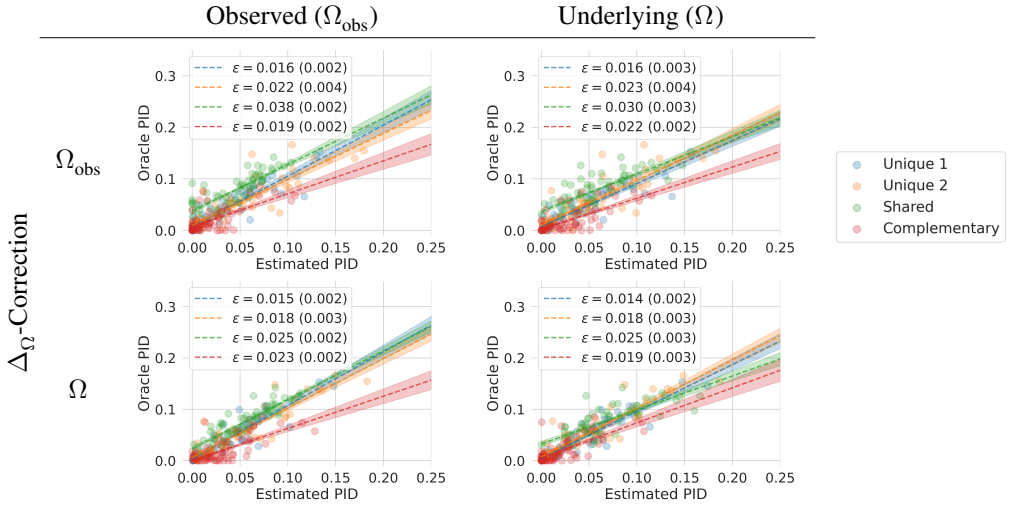

The semi-synthetic experiments examine the effect of enforcing increasing missingness on the performance and information decomposition of UR-FUNNY (Hasan et al., 2019) and hateful memes (Kiela et al., 2020), two foundational real-world datasets used in the multimodal literature for affective computing and content moderation. Table 3 summarizes the effect of enforcing 70% missingness on estimating multimodality informativeness across these datasets, demonstrating the generalizability of our proposed strategy across real-world datasets. Appendix F further illustrates the robustness of the methodology under different levels of missingness in these datasets.

Table 3. Impact of 70% missingness on multimodality information for UR-FUNNY (Hasan et al., 2019) and Hateful Memes (Kiela et al., 2020). Parentheses denote standard deviation across batches.

		AUROC			Information Decomposition			
		Text	Image/Video	Image + Text	Unique Text	Unique Image	Shared	Complementary
UR-FU.	Oracle	0.68 (0.01)	0.60 (0.02)	0.69 (0.02)	0.10 (0.00)	0.02 (0.00)	0.00 (0.00)	0.00 (0.00)
	Observed	0.61 (0.03)	0.54 (0.04)	0.63 (0.03)	0.05 (0.00)	0.00 (0.00)	0.03 (0.00)	0.00 (0.00)
	ICYM^{2}I	0.66 (0.03)	0.57 (0.04)	0.62 (0.04)	0.07 (0.00)	0.00 (0.00)	0.00 (0.00)	0.00 (0.00)
Memes	Oracle	0.71 (0.01)	0.57 (0.01)	0.72 (0.01)	0.09 (0.01)	0.00 (0.00)	0.04 (0.00)	0.05 (0.01)
	Observed	0.68 (0.02)	0.61 (0.02)	0.71 (0.02)	0.13 (0.00)	0.04 (0.00)	0.01 (0.00)	0.00 (0.00)
	ICYM^{2}I	0.67 (0.02)	0.61 (0.02)	0.71 (0.02)	0.10 (0.00)	0.01 (0.00)	0.02 (0.03)	0.03 (0.01)

5.2 Chest radiographs are uninformative over electrocardiograms for structural heart disease detection.

Structural heart disease (SHD) is a set of conditions that affect the heart's physiology and is typically diagnosed using transthoracic echocardiograms (TTEs) (Writing Committee Members et al., 2021). However, TTEs are often underutilized in the United States due to diagnostic stewardship and competing financial incentives (Papolos et al., 2016). Prior work using unimodal models with common modalities in electrocardiograms (ECGs) (Elias et al., 2022; Ulloa-Cerna et al., 2022) and chest radiographs (CXRs) (Bhave et al., 2024) has demonstrated that non-TTE modalities can detect structural heart disease labels. However, CXRs are not systematically collected in conjunction with ECGs, leading to systematic missingness patterns. We, therefore, evaluate ICYM^{2}I on this clinical task to evaluate the informativeness of CXRs in diagnosing SHD, despite its missingness.

Dataset. Our study population consists of a retrospective study gathering 98,397 adult patients who received an ECG and a TTE within one year of each other. The population has 20.56% SHD

prevalence. In this cohort, 12,587 members (12.79%) have recorded CXRs. For subjects with multiple echocardiograms, we select the first TTE to model opportunistic screening with non-TTE modalities. All data were collected from an academic urban medical system between 2008 and 2022. We generate embeddings using modality-specific foundation models–ECG embeddings are generated using ECG-FM (McKeen et al., 2024) and CXR embeddings with ELIXR-C (Xu et al., 2023). Data are split temporally, where subjects with TTEs collected on or after 2018 ($n = 40,734$) are allocated to the test set. All data were de-identified, retrospective, and collected for clinical purposes from an academic hospital system, with approval from the Institutional Review Board. Appendix G contains further details regarding preprocessing and embedding generation.

Results. Table 4 presents the performance of each uni- and multimodal model, along with the associated information decomposition. While both the observed and corrected analyses demonstrate the importance of ECG in modeling SHD, the corrected results raise questions about the information gain associated with CXR. Naive decomposition suggests the unique information in CXRs at about 5% of the total information. However, ICYM^{2}I reduces this unique contribution to 1.8% while increasing estimates of shared information between ECG and CXRs for SHD detection. In contrast to domain knowledge, where ECGs capture electrophysiology while CXRs capture structure and anatomy, two distinct aspects of cardiac health, the corrected complementary and shared results, and low unique information of CXRs suggest that CXRs are not independently useful for SHD diagnosis. Note that our results indicate that the multimodal model performs slightly worse than the unimodal ECG model, reflecting the potential overfitting risk associated with a large number of features.

Table 4. Informativeness of ECG and CXR modalities on model-based structural heart disease detection. Parentheses denote standard deviation across batches ($n = 1024$).

	AUROC			Information Decomposition			
	ECG	CXR	ECG + CXR	Unique ECG	Unique CXR	Shared	Complementary
Observed	0.83 (0.01)	0.72 (0.02)	0.82 (0.01)	0.11 (0.00)	0.01 (0.00)	0.10 (0.00)	-0.00 (0.00)
ICYM^{2}I	0.82 (0.01)	0.73 (0.02)	0.83 (0.01)	0.07 (0.00)	0.01 (0.00)	0.48 (0.00)	0.01 (0.00)

6 Discussion

This work formalizes the issue of missingness when considering multiple modalities. We emphasize that existing works commonly overlook modality missingness by discarding samples with missingness at the curation stage, or implicitly assume that the missingness mechanism remains stable when a model is deployed in the target environment. Our work formalizes this problem and demonstrates its ubiquity in the multimodality literature. Most critically, prior work ignores the fact that any perceived informativeness of a modality may result in increased rates of data collection, inducing different missingness patterns at deployment. Our work, therefore, introduces ICYM^{2}I, a correction to estimate the information gain associated with a *partially observed modality*. Our results demonstrate the methodology's capacity to correct for biases introduced by missingness across synthetic, semi-synthetic, and real-world multimodal datasets. Finally, we evidence the practical utility of this methodology in a healthcare dataset, demonstrating the diverging conclusions that one would reach if ignoring missingness. Our work highlights the critical importance of missingness in multimodal research and urges practitioners to pay particular attention to this issue by systematically *collecting* data with incomplete modalities and carefully *modeling* and *accounting* for missingness to enhance robustness.

Limitations. The key assumption in our work is that modalities are MAR. Practitioners should ensure that this assumption is appropriate for their data. Importantly, MAR is less restrictive than the implicit MCAR assumption made in the multimodal literature. Furthermore, accounting for MNAR requires distributional assumptions that are rarely met or even testable in real-world settings. Additionally, our work is based on Partial Information Decomposition (PID Bertschinger et al. (2014)), which focuses on two input modalities. While theoretical advances to extend to multiple modalities remain an open question (Griffith & Koch, 2014; Kolchinsky, 2022), in practice, practitioners should consider a one-vs-all approach to inform modality informativeness using our method. Like in prior work on PID-based measures of information gain on high-dimensional data (Liang et al., 2023; 2024a), the quality of the representations used may impact the measures returned by ICYM^{2}I. We ensure that our probabilistic estimates are calibrated to mitigate any such challenges.

Ethics statement. Our work demonstrates the impact of missingness on performance estimates in multimodal learning. We demonstrate the utility of our method in a crucial healthcare use case. However, the methodology remains a proof of concept that would require additional testing to be deployed in a real-world context. Our study is approved by the [Anonymized] Institutional Review Board. While beyond the scope of this work, modality completeness is not uniform across demographic subgroups and can manifest in data collection policies, such as differential access to care based on insurance status. Our method could provide important insights into the utility of multimodal predictions in such settings.

Reproducibility statement. Theoretical proofs are provided in Appendix A. All code for applying the proposed ICYM^{2}I and reproducing all synthetic and semi-synthetic results presented in this work will be made publicly available on Github[3]. A summary of the computational resources required to reproduce our results is given in Appendix H.

REFERENCES

Martín Abadi, Ashish Agarwal, Paul Barham, Eugene Brevdo, Zhifeng Chen, Craig Citro, Greg S. Corrado, Andy Davis, Jeffrey Dean, Matthieu Devin, Sanjay Ghemawat, Ian Goodfellow, Andrew Harp, Geoffrey Irving, Michael Isard, Yangqing Jia, Rafal Jozefowicz, Lukasz Kaiser, Manjunath Kudlur, Josh Levenberg, Dandelion Mané, Rajat Monga, Sherry Moore, Derek Murray, Chris Olah, Mike Schuster, Jonathon Shlens, Benoit Steiner, Ilya Sutskever, Kunal Talwar, Paul Tucker, Vincent Vanhoucke, Vijay Vasudevan, Fernanda Viégas, Oriol Vinyals, Pete Warden, Martin Wattenberg, Martin Wicke, Yuan Yu, and Xiaoqiang Zheng. TensorFlow: Large-scale machine learning on heterogeneous systems, 2015. URL https://www.tensorflow.org/. Software available from tensorflow.org.

Tadas Baltrušaitis, Peter Robinson, and Louis-Philippe Morency. Openface: an open source facial behavior analysis toolkit. In *2016 IEEE winter conference on applications of computer vision (WACV)*, pp. 1–10. IEEE, 2016.

Nils Bertschinger, Johannes Rauh, Eckehard Olbrich, Jürgen Jost, and Nihat Ay. Quantifying unique information. *Entropy*, 16(4):2161–2183, 2014.

Shreyas Bhave, Victor Rodriguez, Timothy Poterucha, Simukayi Mutasa, Dwight Aberle, Kathleen M Capaccione, Yibo Chen, Belinda Dsouza, Shifali Dumeer, Jonathan Goldstein, et al. Deep learning to detect left ventricular structural abnormalities in chest x-rays. *European Heart Journal*, pp. ehad782, 2024.

Andreas K Buck, Ken Herrmann, Tom Stargardt, Tobias Dechow, Bernd Joachim Krause, and Jonas Schreyögg. Economic evaluation of pet and pet/ct in oncology: evidence and methodologic approaches. *Journal of nuclear medicine technology*, 38(1):6–17, 2010.

Lei Chen and Chungmin Lee. Predicting audience's laughter during presentations using convolutional neural network. In *Proceedings of the 12th Workshop on Innovative Use of NLP for Building Educational Applications*, pp. 86–90, 2017.

Wen Chen, Pipei Huang, Jiaming Xu, Xin Guo, Cheng Guo, Fei Sun, Chao Li, Andreas Pfadler, Huan Zhao, and Binqiang Zhao. Pog: personalized outfit generation for fashion recommendation at alibaba ifashion. In *Proceedings of the 25th ACM SIGKDD international conference on knowledge discovery & data mining*, pp. 2662–2670, 2019.

Yi-Ting Chen, Jinghao Shi, Zelin Ye, Christoph Mertz, Deva Ramanan, and Shu Kong. Multimodal object detection via probabilistic ensembling. In *European Conference on Computer Vision*, pp. 139–158. Springer, 2022.

Ira Cohen, Fabio Gagliardi Cozman, Nicu Sebe, Marcelo Cesar Cirelo, and Thomas S Huang. Semisupervised learning of classifiers: Theory, algorithms, and their application to human-computer interaction. *IEEE Transactions on Pattern Analysis and Machine Intelligence*, 26(12): 1553–1566, 2004.

[3] https://anonymous.4open.science/r/ICYM2I-BC18/

Noah Cohen Kalafut, Xiang Huang, and Daifeng Wang. Joint variational autoencoders for multimodal imputation and embedding. *Nature machine intelligence*, 5(6):631–642, 2023.

Marco Cuturi. Sinkhorn distances: Lightspeed computation of optimal transport. In C.J. Burges, L. Bottou, M. Welling, Z. Ghahramani, and K.Q. Weinberger (eds.), *Advances in Neural Information Processing Systems*, volume 26. Curran Associates, Inc., 2013. URL https://proceedings.neurips.cc/paper_files/paper/2013/file/af21d0c97db2e27e13572cbf59eb343d-Paper.pdf.

Gilles Degottex, John Kane, Thomas Drugman, Tuomo Raitio, and Stefan Scherer. Covarep—a collaborative voice analysis repository for speech technologies. In *2014 ieee international conference on acoustics, speech and signal processing (icassp)*, pp. 960–964. IEEE, 2014.

Jia Deng, Wei Dong, Richard Socher, Li-Jia Li, Kai Li, and Li Fei-Fei. Imagenet: A large-scale hierarchical image database. In *2009 IEEE conference on computer vision and pattern recognition*, pp. 248–255. Ieee, 2009.

Jacob Devlin, Ming-Wei Chang, Kenton Lee, and Kristina Toutanova. Bert: Pre-training of deep bidirectional transformers for language understanding. In *Proceedings of the 2019 conference of the North American chapter of the association for computational linguistics: human language technologies, volume 1 (long and short papers)*, pp. 4171–4186, 2019.

Pierre Elias, Timothy J Poterucha, Vijay Rajaram, Luca Matos Moller, Victor Rodriguez, Shreyas Bhave, Rebecca T Hahn, Geoffrey Tison, Sean A Abreau, Joshua Barrios, et al. Deep learning electrocardiographic analysis for detection of left-sided valvular heart disease. *Journal of the American College of Cardiology*, 80(6):613–626, 2022.

Jensen Gao, Bidipta Sarkar, Fei Xia, Ted Xiao, Jiajun Wu, Brian Ichter, Anirudha Majumdar, and Dorsa Sadigh. Physically grounded vision-language models for robotic manipulation. In *2024 IEEE International Conference on Robotics and Automation (ICRA)*, pp. 12462–12469. IEEE, 2024.

Chongjian Ge, Junsong Chen, Enze Xie, Zhongdao Wang, Lanqing Hong, Huchuan Lu, Zhenguo Li, and Ping Luo. Metabev: Solving sensor failures for 3d detection and map segmentation. In *Proceedings of the IEEE/CVF International Conference on Computer Vision*, pp. 8721–8731, 2023.

Ary L Goldberger, Luis AN Amaral, Leon Glass, Jeffrey M Hausdorff, Plamen Ch Ivanov, Roger G Mark, Joseph E Mietus, George B Moody, Chung-Kang Peng, and H Eugene Stanley. Physiobank, physiotoolkit, and physionet: components of a new research resource for complex physiologic signals. *circulation*, 101(23):e215–e220, 2000.

Virgil Griffith and Christof Koch. Quantifying synergistic mutual information. In *Guided self-organization: inception*, pp. 159–190. Springer, 2014.

Malte Harder, Christoph Salge, and Daniel Polani. Bivariate measure of redundant information. *Physical Review E—Statistical, Nonlinear, and Soft Matter Physics*, 87(1):012130, 2013.

Md Kamrul Hasan, Wasifur Rahman, AmirAli Bagher Zadeh, Jianyuan Zhong, Md Iftekhar Tanveer, Louis-Philippe Morency, and Mohammed (Ehsan) Hoque. UR-FUNNY: A multimodal language dataset for understanding humor. In Kentaro Inui, Jing Jiang, Vincent Ng, and Xiaojun Wan (eds.), *Proceedings of the 2019 Conference on Empirical Methods in Natural Language Processing and the 9th International Joint Conference on Natural Language Processing (EMNLP-IJCNLP)*, pp. 2046–2056, Hong Kong, China, November 2019. Association for Computational Linguistics. doi: 10.18653/v1/D19-1211.

Kaiming He, Xiangyu Zhang, Shaoqing Ren, and Jian Sun. Deep residual learning for image recognition. In *Proceedings of the IEEE conference on computer vision and pattern recognition*, pp. 770–778, 2016.

Seyedmajid Hosseini, Raju Gottumukkala, Satya Katragadda, Ravi Teja Bhupatiraju, Ziad Ashkar, Christoph W Borst, and Kenneth Cochran. A multimodal sensor dataset for continuous stress detection of nurses in a hospital. *Scientific Data*, 9(1):255, 2022.

Ming Hou, Jiajia Tang, Jianhai Zhang, Wanzeng Kong, and Qibin Zhao. Deep multimodal multilinear fusion with high-order polynomial pooling. *Advances in Neural Information Processing Systems*, 32, 2019.

Arda Inceoglu, Eren Erdal Aksoy, Abdullah Cihan Ak, and Sanem Sariel. Fino-net: A deep multimodal sensor fusion framework for manipulation failure detection. In *2021 IEEE/RSJ international conference on intelligent robots and systems (IROS)*, pp. 6841–6847. IEEE, 2021.

Arda Inceoglu, Eren Erdal Aksoy, and Sanem Sariel. Multimodal detection and classification of robot manipulation failures. *IEEE Robotics and Automation Letters*, 9(2):1396–1403, 2023.

Mimansa Jaiswal and Emily Mower Provost. Privacy enhanced multimodal neural representations for emotion recognition. In *Proceedings of the AAAI Conference on Artificial Intelligence*, volume 34, pp. 7985–7993, 2020.

Neil Jethani, Aahlad Puli, Hao Zhang, Leonid Garber, Lior Jankelson, Yindalon Aphinyanaphongs, and Rajesh Ranganath. New-onset diabetes assessment using artificial intelligence-enhanced electrocardiography. *arXiv preprint arXiv:2205.02900*, 2022.

Alistair EW Johnson, Lucas Bulgarelli, Lu Shen, Alvin Gayles, Ayad Shammout, Steven Horng, Tom J Pollard, Sicheng Hao, Benjamin Moody, Brian Gow, et al. Mimic-iv, a freely accessible electronic health record dataset. *Scientific data*, 10(1):1, 2023.

Douwe Kiela, Hamed Firooz, Aravind Mohan, Vedanuj Goswami, Amanpreet Singh, Pratik Ringshia, and Davide Testuggine. The hateful memes challenge: Detecting hate speech in multimodal memes. *Advances in neural information processing systems*, 33:2611–2624, 2020.

Diederik P Kingma and Jimmy Ba. Adam: A method for stochastic optimization. *arXiv preprint arXiv:1412.6980*, 2014.

Philip A Knight. The sinkhorn–knopp algorithm: convergence and applications. *SIAM Journal on Matrix Analysis and Applications*, 30(1):261–275, 2008.

Artemy Kolchinsky. A novel approach to the partial information decomposition. *Entropy*, 24(3): 403, 2022.

Gueorgi Kossinets. Effects of missing data in social networks. *Social networks*, 28(3):247–268, 2006.

Lien P Le, Thu Nguyen, Michael A Riegler, Pal Halvorsen, and Binh T Nguyen. Multimodal missing data in healthcare: A comprehensive review and future directions. *Computer Science Review*, 56: 100720, 2025.

Kwanhyung Lee, Soojeong Lee, Sangchul Hahn, Heejung Hyun, Edward Choi, Byungeun Ahn, and Joohyung Lee. Learning missing modal electronic health records with unified multi-modal data embedding and modality-aware attention. *arXiv preprint arXiv:2305.02504*, 2023.

Mingcheng Li, Dingkang Yang, Xiao Zhao, Shuaibing Wang, Yan Wang, Kun Yang, Mingyang Sun, Dongliang Kou, Ziyun Qian, and Lihua Zhang. Correlation-decoupled knowledge distillation for multimodal sentiment analysis with incomplete modalities. In *Proceedings of the IEEE/CVF Conference on Computer Vision and Pattern Recognition*, pp. 12458–12468, 2024.

Pin Li, Jeremy MG Taylor, Daniel E Spratt, R Jeffery Karnes, and Matthew J Schipper. Evaluation of predictive model performance of an existing model in the presence of missing data. *Statistics in medicine*, 40(15):3477–3498, 2021.

Zheng Lian, Lan Chen, Licai Sun, Bin Liu, and Jianhua Tao. Gcnet: Graph completion network for incomplete multimodal learning in conversation. *IEEE Transactions on pattern analysis and machine intelligence*, 45:8419–8432, 2023.

Paul Pu Liang, Yiwei Lyu, Xiang Fan, Zetian Wu, Yun Cheng, Jason Wu, Leslie Chen, Peter Wu, Michelle A Lee, Yuke Zhu, et al. Multibench: Multiscale benchmarks for multimodal representation learning. *Advances in neural information processing systems*, 2021(DB1):1, 2021.

Paul Pu Liang, Yun Cheng, Ruslan Salakhutdinov, and Louis-Philippe Morency. Multimodal fusion interactions: A study of human and automatic quantification. In *Proceedings of the 25th International Conference on Multimodal Interaction*, pp. 425–435, 2023.

Paul Pu Liang, Yun Cheng, Xiang Fan, Chun Kai Ling, Suzanne Nie, Richard Chen, Zihao Deng, Nicholas Allen, Randy Auerbach, Faisal Mahmood, et al. Quantifying & modeling multimodal interactions: An information decomposition framework. *Advances in Neural Information Processing Systems*, 36, 2024a.

Paul Pu Liang, Akshay Goindani, Talha Chafekar, Leena Mathur, Haofei Yu, Ruslan Salakhutdinov, and Louis-Philippe Morency. Hemm: Holistic evaluation of multimodal foundation models. *Advances in Neural Information Processing Systems*, 37:42899–42940, 2024b.

Paul Pu Liang, Amir Zadeh, and Louis-Philippe Morency. Foundations & trends in multimodal machine learning: Principles, challenges, and open questions. *ACM Computing Surveys*, 56(10): 1–42, 2024c.

Ronghao Lin and Haifeng Hu. Missmodal: Increasing robustness to missing modality in multimodal sentiment analysis. *Transactions of the Association for Computational Linguistics*, 11:1686–1702, 2023.

Hong Liu, Dong Wei, Donghuan Lu, Jinghan Sun, Liansheng Wang, and Yefeng Zheng. M3ae: Multimodal representation learning for brain tumor segmentation with missing modalities. In *Proceedings of the AAAI conference on artificial intelligence*, volume 37, pp. 1657–1665, 2023a.

Jiashuo Liu, Tianyu Wang, Peng Cui, and Hongseok Namkoong. On the need for a language describing distribution shifts: Illustrations on tabular datasets. *Advances in Neural Information Processing Systems*, 36:51371–51408, 2023b.

Mengmeng Ma, Jian Ren, Long Zhao, Sergey Tulyakov, Cathy Wu, and Xi Peng. Smil: Multimodal learning with severely missing modality. In *Proceedings of the AAAI Conference on Artificial Intelligence*, volume 35, pp. 2302–2310, 2021.

Mengmeng Ma, Jian Ren, Long Zhao, Davide Testuggine, and Xi Peng. Are multimodal transformers robust to missing modality? In *Proceedings of the IEEE/CVF conference on computer vision and pattern recognition*, pp. 18177–18186, 2022.

Yingbo Ma, Mehmet Celepkolu, Kristy Elizabeth Boyer, Collin F Lynch, Eric Wiebe, and Maya Israel. How noisy is too noisy? the impact of data noise on multimodal recognition of confusion and conflict during collaborative learning. In *Proceedings of the 25th International Conference on Multimodal Interaction*, pp. 326–335, 2023.

Daniele Malitesta, Emanuele Rossi, Claudio Pomo, Tommaso Di Noia, and Fragkiskos D Malliaros. Do we really need to drop items with missing modalities in multimodal recommendation? In *Proceedings of the 33rd ACM International Conference on Information and Knowledge Management*, pp. 3943–3948, 2024.

William McGill. Multivariate information transmission. *Transactions of the IRE Professional Group on Information Theory*, 4(4):93–111, 1954.

Kaden McKeen, Laura Oliva, Sameer Masood, Augustin Toma, Barry Rubin, and Bo Wang. Ecg-fm: An open electrocardiogram foundation model. *arXiv preprint arXiv:2408.05178*, 2024.

Antoine Miech, Dimitri Zhukov, Jean-Baptiste Alayrac, Makarand Tapaswi, Ivan Laptev, and Josef Sivic. Howto100m: Learning a text-video embedding by watching hundred million narrated video clips. In *Proceedings of the IEEE/CVF international conference on computer vision*, pp. 2630–2640, 2019.

Karthika Mohan and Judea Pearl. Graphical models for processing missing data. *Journal of the American Statistical Association*, 116(534):1023–1037, 2021.

Jiquan Ngiam, Aditya Khosla, Mingyu Kim, Juhan Nam, Honglak Lee, Andrew Y Ng, et al. Multimodal deep learning. In *ICML*, volume 11, pp. 689–696, 2011.

Changdae Oh, Zhen Fang, Shawn Im, Xuefeng Du, and Yixuan Li. Understanding multimodal llms under distribution shifts: An information-theoretic approach. *arXiv preprint arXiv:2502.00577*, 2025.

Alexander Papolos, Jagat Narula, Chirag Bavishi, Farooq A Chaudhry, and Partho P Sengupta. Us hospital use of echocardiography: insights from the nationwide inpatient sample. *Journal of the American College of Cardiology*, 67(5):502–511, 2016.

Adam Paszke, Sam Gross, Francisco Massa, Adam Lerer, James Bradbury, Gregory Chanan, Trevor Killeen, Zeming Lin, Natalia Gimelshein, Luca Antiga, et al. Pytorch: An imperative style, high-performance deep learning library. *Advances in neural information processing systems*, 32, 2019.

Jeffrey Pennington, Richard Socher, and Christopher D Manning. Glove: Global vectors for word representation. In *Proceedings of the 2014 conference on empirical methods in natural language processing (EMNLP)*, pp. 1532–1543, 2014.

Sam Perochon, J Matias Di Martino, Kimberly LH Carpenter, Scott Compton, Naomi Davis, Brian Eichner, Steven Espinosa, Lauren Franz, Pradeep Raj Krishnappa Babu, Guillermo Sapiro, et al. Early detection of autism using digital behavioral phenotyping. *Nature Medicine*, 29(10):2489–2497, 2023.

Matthew Phelan, Nrupen A Bhavsar, and Benjamin A Goldstein. Illustrating informed presence bias in electronic health records data: how patient interactions with a health system can impact inference. *EGEMs*, 5(1), 2017.

Stephen M Pizer, E Philip Amburn, John D Austin, Robert Cromartie, Ari Geselowitz, Trey Greer, Bart ter Haar Romeny, John B Zimmerman, and Karel Zuiderveld. Adaptive histogram equalization and its variations. *Computer vision, graphics, and image processing*, 39(3):355–368, 1987.

M. Reyna, N. Sadr, A. Gu, E. A. Perez Alday, C. Liu, S. Seyedi, A. Shah, and G. Clifford. Will two do? varying dimensions in electrocardiography: The physionet/computing in cardiology challenge 2021 (version 1.0.3). *PhysioNet*, 2022. doi: 10.13026/34va-7q14.

Matthew A Reyna, Nadi Sadr, Erick A Perez Alday, Annie Gu, Amit J Shah, Chad Robichaux, Ali Bahrami Rad, Andoni Elola, Salman Seyedi, Sardar Ansari, et al. Will two do? varying dimensions in electrocardiography: the physionet/computing in cardiology challenge 2021. In *2021 computing in cardiology (CinC)*, volume 48, pp. 1–4. IEEE, 2021.

James M Robins, Andrea Rotnitzky, and Lue Ping Zhao. Estimation of regression coefficients when some regressors are not always observed. *Journal of the American statistical Association*, 89 (427):846–866, 1994.

Donald B Rubin. Inference and missing data. *Biometrika*, 63(3):581–592, 1976.

Christoph Schuhmann, Romain Beaumont, Richard Vencu, Cade Gordon, Ross Wightman, Mehdi Cherti, Theo Coombes, Aarush Katta, Clayton Mullis, Mitchell Wortsman, et al. Laion-5b: An open large-scale dataset for training next generation image-text models. *Advances in neural information processing systems*, 35:25278–25294, 2022.

Dhruv Shah, Błażej Osiński, Sergey Levine, et al. Lm-nav: Robotic navigation with large pre-trained models of language, vision, and action. In *Conference on robot learning*, pp. 492–504. PMLR, 2023.

Piyush Sharma, Nan Ding, Sebastian Goodman, and Radu Soricut. Conceptual captions: A cleaned, hypernymed, image alt-text dataset for automatic image captioning. In *Proceedings of the 56th Annual Meeting of the Association for Computational Linguistics (Volume 1: Long Papers)*, pp. 2556–2565, 2018.

Richard Sinkhorn and Paul Knopp. Concerning nonnegative matrices and doubly stochastic matrices. *Pacific Journal of Mathematics*, 21(2):343–348, 1967.

Elizabeth A Stuart. Matching methods for causal inference: A review and a look forward. *Statistical science: a review journal of the Institute of Mathematical Statistics*, 25(1), 2010.

Han Te Sun. Multiple mutual informations and multiple interactions in frequency data. *Inf. Control*, 46:26–45, 1980.

Luan Tran, Xiaoming Liu, Jiayu Zhou, and Rong Jin. Missing modalities imputation via cascaded residual autoencoder. In *Proceedings of the IEEE conference on computer vision and pattern recognition*, pp. 1405–1414, 2017.

Tao Tu, Shekoofeh Azizi, Danny Driess, Mike Schaekermann, Mohamed Amin, Pi-Chuan Chang, Andrew Carroll, Charles Lau, Ryutaro Tanno, Ira Ktena, et al. Towards generalist biomedical ai. *NEJM AI*, 1(3):AIoa2300138, 2024.

Alvaro E Ulloa-Cerna, Linyuan Jing, John M Pfeifer, Sushravya Raghunath, Jeffrey A Ruhl, Daniel B Rocha, Joseph B Leader, Noah Zimmerman, Greg Lee, Steven R Steinhubl, et al. Rechommend: an ecg-based machine learning approach for identifying patients at increased risk of undiagnosed structural heart disease detectable by echocardiography. *Circulation*, 146(1):36–47, 2022.

Aayush Atul Verma, Amir Saeidi, Shamanthak Hegde, Ajay Therala, Fenil Denish Bardoliya, Nagaraju Machavarapu, Shri Ajay Kumar Ravindhiran, Srija Malyala, Agneet Chatterjee, Yezhou Yang, et al. Evaluating multimodal large language models across distribution shifts and augmentations. In *Proceedings of the IEEE/CVF Conference on Computer Vision and Pattern Recognition*, pp. 5314–5324, 2024.

Qi Wang, Liang Zhan, Paul Thompson, and Jiayu Zhou. Multimodal learning with incomplete modalities by knowledge distillation. In *Proceedings of the 26th ACM SIGKDD International Conference on Knowledge Discovery & Data Mining*, pp. 1828–1838, 2020a.

Weiyao Wang, Du Tran, and Matt Feiszli. What makes training multi-modal classification networks hard? In *Proceedings of the IEEE/CVF conference on computer vision and pattern recognition*, pp. 12695–12705, 2020b.

Paul L Williams and Randall D Beer. Nonnegative decomposition of multivariate information. *arXiv preprint arXiv:1004.2515*, 2010.

Sangmin Woo, Sumin Lee, Yeonju Park, Muhammad Adi Nugroho, and Changick Kim. Towards good practices for missing modality robust action recognition. In *Proceedings of the AAAI Conference on Artificial Intelligence*, volume 37, pp. 2776–2784, 2023.

Catherine M Writing Committee Members, Otto, Rick A Nishimura, Robert O Bonow, Blase A Carabello, John P Erwin III, Federico Gentile, Hani Jneid, Eric V Krieger, Michael Mack, et al. 2020 acc/aha guideline for the management of patients with valvular heart disease: a report of the american college of cardiology/american heart association joint committee on clinical practice guidelines. *Journal of the American College of Cardiology*, 77(4):e25–e197, 2021.

Renjie Wu, Hu Wang, Hsiang-Ting Chen, and Gustavo Carneiro. Deep multimodal learning with missing modality: A survey. *arXiv preprint arXiv:2409.07825*, 2024.

Aaron D Wyner. A definition of conditional mutual information for arbitrary ensembles. *Information and Control*, 38(1):51–59, 1978.

Shawn Xu, Lin Yang, Christopher Kelly, Marcin Sieniek, Timo Kohlberger, Martin Ma, Wei-Hung Weng, Atilla Kiraly, Sahar Kazemzadeh, Zakkai Melamed, et al. Elixr: Towards a general purpose x-ray artificial intelligence system through alignment of large language models and radiology vision encoders. *arXiv preprint arXiv:2308.01317*, 2023.

Yihao Xue, Siddharth Joshi, Dang Nguyen, and Baharan Mirzasoleiman. Understanding the robustness of multi-modal contrastive learning to distribution shift. In *The Twelfth International Conference on Learning Representations*, 2024. URL https://openreview.net/forum?id=rtl4XnJYBh.

Jiahong Yuan, Mark Liberman, et al. Speaker identification on the scotus corpus. *Journal of the Acoustical Society of America*, 123(5):3878, 2008.

Amir Zadeh, Minghai Chen, Soujanya Poria, Erik Cambria, and Louis-Philippe Morency. Tensor fusion network for multimodal sentiment analysis. *arXiv preprint arXiv:1707.07250*, 2017.

Jiandian Zeng, Jiantao Zhou, and Tianyi Liu. Mitigating inconsistencies in multimodal sentiment analysis under uncertain missing modalities. In *Proceedings of the 2022 conference on empirical methods in natural language processing*, pp. 2924–2934, 2022.

Yuexiang Zhai, Shengbang Tong, Xiao Li, Mu Cai, Qing Qu, Yong Jae Lee, and Yi Ma. Investigating the catastrophic forgetting in multimodal large language model fine-tuning. In *Conference on Parsimony and Learning*, pp. 202–227. PMLR, 2024.

Haoran Zhang, Harvineet Singh, Marzyeh Ghassemi, and Shalmali Joshi. "Why did the model fail?": Attributing model performance changes to distribution shifts. In Andreas Krause, Emma Brunskill, Kyunghyun Cho, Barbara Engelhardt, Sivan Sabato, and Jonathan Scarlett (eds.), *Proceedings of the 40th International Conference on Machine Learning*, volume 202 of *Proceedings of Machine Learning Research*, pp. 41550–41578. PMLR, 23–29 Jul 2023.

Peng-Fei Zhang, Yang Li, Zi Huang, and Hongzhi Yin. Privacy protection in deep multi-modal retrieval. In *Proceedings of the 44th International ACM SIGIR Conference on Research and Development in Information Retrieval*, pp. 634–643, 2021.

Yuhui Zhang, Alyssa Unell, Xiaohan Wang, Dhruba Ghosh, Yuchang Su, Ludwig Schmidt, and Serena Yeung-Levy. Why are visually-grounded language models bad at image classification? In *The Thirty-eighth Annual Conference on Neural Information Processing Systems*, 2024. URL https://openreview.net/forum?id=MwmmBg1VYg.

Guanglin Zhou, Zhongyi Han, Shiming Chen, Biwei Huang, Liming Zhu, Salman Khan, Xin Gao, and Lina Yao. Adapting large multimodal models to distribution shifts: The role of in-context learning. *arXiv preprint arXiv:2405.12217*, 2024.

Helen Zhou, Sivaraman Balakrishnan, and Zachary Lipton. Domain adaptation under missingness shift. In *International Conference on Artificial Intelligence and Statistics*, pp. 9577–9606. PMLR, 2023.

Tongxue Zhou, Pierre Vera, Stéphane Canu, and Su Ruan. Missing data imputation via conditional generator and correlation learning for multimodal brain tumor segmentation. *Pattern Recognition Letters*, 158:125–132, 2022.

A PROOFS

This section provides the proofs for Lemma 1 and Lemma 2.

Lemma 1. *The separable loss function computed on the observed data $l_{\Omega_{obs}}(x_1, x_2, y)$ can be reweighted to approximate the target loss $l_\Omega(x_1, x_2, y)$ as follows:*

$$l_\Omega(x_1, x_2, y) = \frac{1}{1 - p_\Omega(m_1, m_2, m_y \mid C)} \, l_{\Omega_{obs}}(x_1, x_2, y)$$

where $p_\Omega(m_1, m_2, m_y \mid C)$ is the probability of missingness, given the covariates C.

Proof. The proof is analogous to that of Lemma 2, which we show in detail, for any separable loss function $l(x_1, x_2, y)$. □

Lemma 2.

$$I_\Omega(Y : (X_1, X_2)) = \mathbb{E}_{\substack{x_1, x_2 \sim p_{\Omega_{obs}}(x_1, x_2) \\ y \sim p_\Omega(y \mid x_1, x_2)}} \left[\frac{1 - p(m_1, m_2)}{1 - p(m_1, m_2 | x_1, x_2, y)} \log \left(\frac{p_\Omega(x_1, x_2, y)}{p_\Omega(x_1, x_2) p_\Omega(y)} \right) \right]$$

Proof. Let $m = (m_1, m_2)$,

$$\begin{aligned}
& I_\Omega(Y : (X_1, X_2)) \\
&= \mathbb{E}_\Omega \left[\log \left(\frac{p_\Omega(x_1, x_2, y)}{p_\Omega(x_1, x_2) p_\Omega(y)} \right) \right] \\
&= \mathbb{E}_{\substack{x_1, x_2 \sim p_{\Omega_{\text{obs}}}(x_1, x_2) \\ y \sim p_\Omega(y \mid x_1, x_2)}} \left[\frac{p_\Omega(x_1, x_2, y)}{p_{\Omega_{\text{obs}}}(x_1, x_2, y)} \log \left(\frac{p_\Omega(x_1, x_2, y)}{p_\Omega(x_1, x_2) p_\Omega(y)} \right) \right] \\
&= \mathbb{E}_{\substack{x_1, x_2 \sim p_{\Omega_{\text{obs}}}(x_1, x_2) \\ y \sim p_\Omega(y \mid x_1, x_2)}} \left[\frac{p_\Omega(x_1, x_2, y)}{p_\Omega(x_1, x_2, y \mid m = 0)} \log \left(\frac{p_\Omega(x_1, x_2, y)}{p_\Omega(x_1, x_2) p_\Omega(y)} \right) \right] \\
&= \mathbb{E}_{\substack{x_1, x_2 \sim p_{\Omega_{\text{obs}}}(x_1, x_2) \\ y \sim p_\Omega(y \mid x_1, x_2)}} \left[\frac{p_\Omega(x_1, x_2, y)}{\frac{p(m=0 \mid x_1, x_2, y) p_\Omega(x_1, x_2, y)}{p(m=0)}} \log \left(\frac{p_\Omega(x_1, x_2, y)}{p_\Omega(x_1, x_2) p_\Omega(y)} \right) \right] \\
&= \mathbb{E}_{\substack{x_1, x_2 \sim p_{\Omega_{\text{obs}}}(x_1, x_2) \\ y \sim p_\Omega(y \mid x_1, x_2)}} \left[\frac{1 - p(m = 1)}{1 - p(m = 1 | x_1, x_2, y)} \log \left(\frac{p_\Omega(x_1, x_2, y)}{p_\Omega(x_1, x_2) p_\Omega(y)} \right) \right]
\end{aligned}$$

□

That is, to estimate the mutual information under the true data distribution, we adjust for the shift in $p_{\Omega_{\text{obs}}}(x_1, x_2) \mapsto p_\Omega(x_1, x_2)$ and sample y from the IPW-adjusted (parametrized approximations) of $p_\Omega(y \mid x_1, x_2)$.

B PARTIAL INFORMATION DECOMPOSITION (PID)

Partial information decomposition (PID Williams & Beer (2010)) consists in decomposing the total mutual information (McGill, 1954; Te Sun, 1980) between a target variable and two input variables into information about the target variable that both input variables share ("Shared" information), only one input variable has ("Unique" information) and emerges from the interactions of both ("Complementary" information). Bertschinger et al. (2014) introduces bounds for these, reiterated below. In this Appendix, we express these bounds as entropy. First, Table 5 summarizes the notations used in the literature and those used in our work.

Table 5. Quantities and associated variables. Note that the four information measures are approximations.

Quantity	Bertschinger	ICYM^{2}I
Input Variable 1	Y	X_1
Input Variable 2	Z	X_2
Target Variable	X	Y
Redundant / Shared Information	$\widetilde{SI}(X:Y:Z)$	$\widetilde{SI}(Y:X_1;X_2)$
Unique Information (Input Variable 1)	$\widetilde{UI}(X:Y\backslash Z)$	$\widetilde{UI}(Y:X_1\backslash X_2)$
Unique Information (Input Variable 2)	$\widetilde{UI}(X:Z\backslash Y)$	$\widetilde{UI}(Y:X_2\backslash X_1)$
Synergistic / Complementary Information	$\widetilde{CI}(X:Y;Z)$	$\widetilde{CI}(Y:X_1;X_2)$

PID decomposition of the three-way mutual information $I(Y:(X_1,X_2))$ results in the quantities of interest as follows:

$$I(Y:(X_1,X_2)) = \underbrace{SI(Y:X_1;X_2)}_{\text{Shared}} + \underbrace{UI(Y:X_1\backslash X_2)}_{\text{Unique 1}} + \underbrace{UI(Y:X_2\backslash X_1)}_{\text{Unique 2}} + \underbrace{CI(Y:X_1;X_2)}_{\text{Complementary}}$$

Bertschinger et al. (2014) provides the following bounds on each of these quantities:

$$\begin{aligned}
\widetilde{SI}(Y:X_1;X_2) &= \max_{q\in\Delta_\Omega} CoI_q(Y;X_1;X_2) \\
&= \max_{q\in\Delta_\Omega} [I_q(Y:X_1) - I_q(Y:X_1|X_2)] \\
&= \max_{q\in\Delta_\Omega} [[I_q(Y:(X_1,X_2)) - I_q(Y:X_2|X_1)] - I_q(Y:X_1|X_2)] \\
&= \max_{q\in\Delta_\Omega} [I_q(Y:(X_1,X_2)) - [I_q(Y:X_2|X_1) + I_q(Y:X_1|X_2)]] \\
\widetilde{UI}(Y:X_1\backslash X_2) &= \min_{q\in\Delta_\Omega} I_q(Y:X_1|X_2) \\
&= \min_{q\in\Delta_\Omega} [I_q(Y:(X_1,X_2)) - I_q(Y:X_2)] \\
\widetilde{UI}(Y:X_2\backslash X_1) &= \min_{q\in\Delta_\Omega} I_q(Y:X_2|X_1) \\
&= \min_{q\in\Delta_\Omega} [I_q(Y:(X_1,X_2)) - I_q(Y:X_1)] \\
\widetilde{CI}(Y:X_1;X_2) &= I_\Omega(Y:(X_1,X_2)) - \min_{q\in\Delta_\Omega} I_q(Y:(X_1,X_2))
\end{aligned}$$

In this context, Bertschinger et al. (2014) demonstrates that solving the optimization for $q \in \Delta_\Omega$ that satisfies one of the four conditions above or the bound for conditional entropy, $\widetilde{H}$ formalized in (5), is sufficient to obtain all the quantities of interest.

$$\widetilde{H}(Y|X_1,X_2) = \max_{q\in\Delta_\Omega} H_q(Y|X_1,X_2) \tag{5}$$

Formulating PID quantities in terms of entropy Remember that entropy $H(\cdot)$ is defined for general distributions of X and Y as follows:

$$\begin{aligned} H(X) &:= -\sum_{x\in\mathcal{X}} p(x)\log p(x) \\ H(Y,X) &:= -\sum_{x\in\mathcal{X},y\in\mathcal{Y}} p(y,x)\log\left(p(y,x)\right) \\ H(Y|X) &:= -\sum_{x\in\mathcal{X},y\in\mathcal{Y}} p(y,x)\log\left(\frac{p(y,x)}{p(x)}\right) \\ &= H(Y,X) - H(X) \end{aligned}$$

Using these notations, the mutual information $I(\cdot)$ can be defined as:

$$\begin{aligned} I(Y:X) &:= H(X) - H(X|Y) \\ &= H(X) + H(Y) - H(Y,X) \\ I(Y:X_2|X_1) &:= H(Y,X_1) + H(X_1,X_2) - H(Y,X_1,X_2) - H(X_1) \end{aligned}$$

The previous quantities of interest can then be derived as:

$$\begin{aligned} I(Y:(X_1,X_2)) &:= I(Y:X_1) + I(Y:X_2|X_1) \\ &= \underbrace{H(Y) + \cancel{H(X_1)} - \cancel{H(Y,X_1)}}_{I(Y:X_1)} + \underbrace{\cancel{H(Y,X_1)} + H(X_1,X_2) - H(Y,X_1,X_2) - \cancel{H(X_1)}}_{I(Y:X_2|X_1)} \\ &= H(Y) + H(X_1,X_2) - H(Y,X_1,X_2) \end{aligned}$$

where the first equation comes from the chain rule of mutual information (Wyner, 1978).

Similarly, we can get the expression for co-information $CoI(Y;X_1;X_2)$:

$$\begin{aligned} CoI(Y;X_1;X_2) =& I(Y:X_1) + I(Y:X_2) - I(Y:(X_1,X_2)) \\ =& \underbrace{[H(Y) - H(Y|X_1)]}_{I(Y:X_1)} + \underbrace{[H(Y) - H(Y|X_2)]}_{I(Y:X_2)} \\ & \underbrace{[H(Y) + H(X_1,X_2) - H(Y,X_1,X_2)]}_{I(Y:(X_1,X_2))} \\ =& [H(Y) - [H(Y,X_1) - H(X_1)]] + [\cancel{H(Y)} - [H(Y,X_2) - H(X_2)]] \\ & - [\cancel{H(Y)} + H(X_1,X_2) - H(Y,X_1,X_2)] \\ =& H(Y) + H(X_1) + H(X_2) \\ & - [H(X_1,X_2) + H(Y,X_1) + H(Y,X_2)] \\ & + H(Y,X_1,X_2) \end{aligned}$$

The PID bounds can then be expressed in terms of entropy:

$$
\begin{aligned}
\widetilde{SI}(Y:X_1;X_2) &= \max_{q\in\Delta_\Omega} CoI_q(Y;X_1;X_2) \\
&= \max_{q\in\Delta_\Omega} [H_q(Y) + H_q(X_1) + H_q(X_2) \\
&\quad - [H_q(X_1,X_2) + H_q(Y,X_1) + H_q(Y,X_2)] + H_q(Y,X_1,X_2)] \\
\widetilde{UI}(Y:X_1\backslash X_2) &= \min_{q\in\Delta_\Omega} I_q(Y:X_1|X_2) \\
&= \min_{q\in\Delta_\Omega} [H_q(Y,X_2) + H_q(X_1,X_2) - H_q(Y,X_1,X_2) - H_q(X_2)] \\
\widetilde{UI}(Y:X_2\backslash X_1) &= \min_{q\in\Delta_\Omega} I_q(Y:X_2|X_1) \\
&= \min_{q\in\Delta_\Omega} [H_q(Y,X_1) + H_q(X_1,X_2) - H_q(Y,X_1,X_2) - H_q(X_1)] \\
\widetilde{CI}(Y:X_1;X_2) &= I_\Omega(Y:(X_1,X_2)) - \min_{q\in\Delta_\Omega} I_q(Y:(X_1,X_2)) \\
&= [H_\Omega(Y) + H_\Omega(X_1,X_2) - H_\Omega(Y,X_1,X_2)] \\
&\quad - \min_{q\in\Delta_\Omega} [H_q(Y) + H_q(X_1,X_2) - H_q(Y,X_1,X_2)]
\end{aligned}
$$

where $H_q(\cdot)$ and $H_\Omega(\cdot)$ is the entropy of a variable under probability distributions q and Ω, respectively.

C ICYM^{2}I-PID

Table 6. ICYM^{2}I: Inverse probability weighting-adjusted multimodal training and evaluation under missingness shift.

		Evaluation distribution	
		Observed Ω_{obs} 	Underlying Ω 
Training		Current practice	IPW-adjusted evaluation alone
		IPW-adjusted training alone	ICYM^{2}I (IPW-adjusted training and evaluation)

Let $\text{IPW}_q(p)$ denote IPW reweighting to correct $p \mapsto q$ using samples from p. We use the following projection set to operationalize PID-bound estimation:

$$
\begin{aligned}
&\Delta_{\Omega}^{\text{ICYM}^2\text{I}} \\
\approx&\{q \propto \exp(f_1(x_1) \cdot f_2(x_2)) : q(X_i = x_i, Y = y) = p_{\Omega\,\phi}(y, x_i)\,\forall x_i \in \mathcal{X}_i, y \in \mathcal{Y}, i \in \{1, 2\}\} \\
=&\{q \propto \exp(f_1(x_1) \cdot f_2(x_2)) : q(X_i = x_i, Y = y) = \text{IPW}_{p_{\Omega\,\phi}}(p_{\Omega_{\text{obs}}\,\phi}(y, x_i))\,\forall x_i \in \mathcal{X}_i, y \in \mathcal{Y}, i \in \{1, 2\}\}
\end{aligned}
$$

Note that this differs from prior works Liang et al. (2024a) that have used:

$$\Delta_{\Omega} \approx \{q \propto \exp(f_1(x_1) \cdot f_2(x_2)) : q(x_i, y) = \Omega_{\text{obs}\,\phi}(x_i, y)\,\forall x_i \in \mathcal{X}_i, y \in \mathcal{Y}, i \in \{1, 2\}\}$$

To further improve the robustness of $p_{\Omega_{\text{obs}}}(y, x_i) \approx p_{\Omega_{\text{obs}}\,\phi}(y, x_i)$, we optionally leverage both the unimodal and multimodal estimations, i.e., the unimodal and multimodal prediction models to enforce:

$$\sum_{x_{\neg i}} f_\phi(y \mid x_1, x_2) p_{\Omega_{\text{obs}}}(x_1, x_2) = \hat{f}_\phi(y \mid x_i) p_{\Omega_{\text{obs}}}(x_i),$$

where $\hat{f}$ is obtained by adding the smallest amount of noise to $f_\phi(y \mid x_i) \approx p_{\Omega_{\text{obs}}}(y \mid x_i)$ to ensure that the joint probabilities from the parametrized unimodal and multimodal models match exactly. This optimization did not improve PID values' recovery.

We summarize our proposed auto-differentiable PID algorithm with IPW-based correction in Algorithm 1.

Algorithm 1 ICYM^{2}I-PID

Require: $X_1, X_2, Y \sim p_{\Omega_{\text{obs}}}$
1: # Adjust $\Omega_{\text{obs}} \mapsto \Omega$.
2: Estimate missingness mechanisms $p_{\Omega\,\phi}(M_1, M_2, M_Y \mid C)$ for IPW.
3: Estimate corrected unimodal and multimodal models by training with weighting IPW-loss: $f_\phi(y \mid x_i) \approx p_\Omega(y \mid x_i)$, $\forall i \in \{1, 2\}$, and $f_\phi(y \mid x_1, x_2) \approx p_\Omega(y \mid x_1, x_2)$.
4: # Drop subscript ϕ from f_ϕ for clarity.
5: Initialize parameterizations θ for q: $f_i(y \mid x_i)$, $\forall i \in \{1, 2\}$.
6: $q_\theta(y \mid x_1, x_2) \leftarrow \exp\left(f_1(y \mid x_1) f_2(y \mid x_2)^T\right)$
7: **while** not converged **do**
8: **for** samples in batch **do**
9: # Project onto $\Delta_\Omega^{\text{ICYM}^2\text{I}}$.
10: $q_\theta(y \mid x_1, x_2) \leftarrow \texttt{SINKHORN-KNOPP}(q_\theta(y \mid x_1, x_2), \{p(y, x_i)\}_{i=1}^2)$.
11: Estimate the loss $I_q(Y : (X_1, X_2))$ as a batch sample mean.
12: $\theta \leftarrow \theta - \nabla_\theta I_q(Y : (X_1, X_2))$.
13: **end for**
14: **end while**
 # Estimate mutual information under p_Ω.
15: Estimate $I_\Omega(Y : (X_1, X_2))$, and $I_\Omega(Y : X_i)$, $\forall i \in \{1, 2\}$ using adjustment in Appendix A.
16: $PID(\Omega) \leftarrow (\widetilde{CI}(Y : X_1; X_2), \widetilde{SI}(Y : X_1; X_2), \widetilde{UI}(Y : X_1 \backslash X_2), \widetilde{UI}(Y : X_2 \backslash X_1))$
17: **return** $PID(\Omega)$

The traditional `SINKHORN-KNOPP` algorithm updates a matrix to enforce its marginals to be unit vectors. In our work, we adapt the algorithm to enforce the marginals to match p_Ω-marginals, ensuring that $q_\theta(\cdot) \in \Delta_\Omega$. To ensure proper gradient propagation and reduce memory use, we use the unrolled `SINKHORN-KNOPP` (Sinkhorn & Knopp, 1967; Cuturi, 2013) algorithm. In the following, we use subscripts q_{x_1,x_2} to denote $q_\theta(y, x_1, x_2)$ and p_{x_i} to denote $p_\phi(y, x_i)$. The algorithm is detailed below:

Algorithm 2 Unrolled `SINKHORN-KNOPP` update

Require: $q_{x_1x_2}, p_{x_1}, p_{x_2}$, tolerance `atol`
$q_{x_1} \leftarrow \sum_{x_2} q_{x_1x_2}$
$q_{x_2} \leftarrow \sum_{x_1} q_{x_1x_2}$
while do
 # Avoid update if both exit conditions have been met.
 if $\left|\frac{q_{x_1} - p_{x_1}}{p_{x_1}}\right| \leq \texttt{atol}$ **and** $\left|\frac{q_{x_2} - p_{x_2}}{p_{x_2}}\right| \leq \texttt{atol}$ **then**
  return $q_{x_1x_2}$
 end if
 # Update marginal.
 $q_{x_1x_2} \leftarrow \frac{q_{x_1x_2}}{q_{x_2}} \cdot p_{x_2}$
 $q_{x_1} \leftarrow \sum_{x_2} q_{x_1x_2}$
 # If the other marginal still matches, done.
 if $\left|\frac{q_{x_1} - p_{x_1}}{p_{x_1}}\right| \leq \texttt{atol}$ **then**
  return $q_{x_1x_2}$
 end if
 # Repeat for the other marginal.
 $q_{x_1x_2} \leftarrow \frac{q_{x_1x_2}}{q_{x_1}} \cdot p_{x_1}$
 $q_{x_2} \leftarrow \sum_{x_1} q_{x_1x_2}$
 if $\left|\frac{q_{x_2} - p_{x_2}}{p_{x_2}}\right| \leq \texttt{atol}$ **then**
  return $q_{x_1x_2}$
 end if
end while

D BIT-WISE LOGITS

In this section, we perform a sensitivity analysis of the logit setting presented in Section 4.1 under two additional missingness patterns: MCAR (Missing Completely at Random) and MNAR (Missing Not at Random). In this setting, we fit a logistic regression to estimate the probability of missingness on the observed modality, which is then used to estimate the IPW. The performance estimates and PID for these two missingness processes are illustrated in Tables 7 and 8.

Since MCAR does not result in a distribution shift, one expects the same performance estimates for both the full and observed populations. Furthermore, in this setting, the IPW correction corresponds to a constant value, as any point has the same probability of observing both modalities. This correction also results in no change in performance estimates.

On the contrary, MNAR patterns do not guarantee similar behavior. Particularly, this missingness process may result in a distribution shift that cannot be assessed or accounted for without assumptions about the data distribution, as one does not observe the covariates that impact the missingness process. The results demonstrate that both the observed and corrected strategies result in biased estimates.

Table 7. Impact of missingness on multimodality information for bitwise logic operators under MCAR. Parentheses denote standard deviation across batches.

		AUROC			Information Decomposition			
		X_1	X_2	$X_1 + X_2$	Unique 1	Unique 2	Shared	Complementary
AND	Oracle	0.83 (0.01)	0.84 (0.01)	1.00 (0.00)	0.05 (0.00)	0.03 (0.00)	0.26 (0.00)	0.47 (0.00)
	Observed	0.83 (0.01)	0.83 (0.01)	1.00 (0.00)	0.05 (0.00)	0.03 (0.00)	0.23 (0.00)	0.52 (0.00)
	ICYM^{2}I	0.83 (0.01)	0.85 (0.01)	1.00 (0.00)	0.03 (0.00)	0.06 (0.00)	0.27 (0.00)	0.44 (0.00)
OR	Oracle	0.84 (0.01)	0.83 (0.01)	1.00 (0.00)	0.04 (0.00)	0.05 (0.00)	0.27 (0.00)	0.46 (0.00)
	Observed	0.84 (0.01)	0.84 (0.01)	1.00 (0.00)	0.06 (0.00)	0.03 (0.00)	0.25 (0.00)	0.51 (0.00)
	ICYM^{2}I	0.85 (0.01)	0.83 (0.01)	1.00 (0.00)	0.06 (0.00)	0.02 (0.00)	0.25 (0.00)	0.51 (0.00)
XOR	Oracle	0.51 (0.02)	0.49 (0.01)	1.00 (0.00)	0.00 (0.00)	0.00 (0.00)	0.00 (0.00)	0.99 (0.00)
	Observed	0.51 (0.02)	0.50 (0.02)	1.00 (0.00)	0.00 (0.00)	0.00 (0.00)	0.00 (0.00)	0.95 (0.00)
	ICYM^{2}I	0.51 (0.02)	0.51 (0.02)	1.00 (0.00)	0.00 (0.00)	0.00 (0.00)	0.00 (0.00)	0.95 (0.00)

Table 8. Impact of missingness on multimodality information for bitwise logic operators under MNAR. Parentheses denote standard deviation across batches.

		AUROC			Information Decomposition			
		X_1	X_2	$X_1 + X_2$	Unique 1	Unique 2	Shared	Complementary
AND	Oracle	0.83 (0.01)	0.84 (0.01)	1.00 (0.00)	0.05 (0.00)	0.03 (0.00)	0.26 (0.00)	0.47 (0.00)
	Observed	0.93 (0.01)	0.67 (0.01)	1.00 (0.00)	0.45 (0.00)	0.00 (0.00)	0.17 (0.00)	0.33 (0.00)
	ICYM^{2}I	0.93 (0.01)	0.67 (0.01)	1.00 (0.00)	0.45 (0.00)	0.00 (0.00)	0.17 (0.00)	0.33 (0.00)
OR	Oracle	0.84 (0.01)	0.83 (0.01)	1.00 (0.00)	0.04 (0.00)	0.05 (0.00)	0.27 (0.00)	0.46 (0.00)
	Observed	0.78 (0.01)	0.95 (0.01)	1.00 (0.00)	0.00 (0.00)	0.17 (0.00)	0.11 (0.00)	0.23 (0.00)
	ICYM^{2}I	0.78 (0.01)	0.95 (0.01)	1.00 (0.00)	0.00 (0.00)	0.17 (0.00)	0.11 (0.00)	0.23 (0.00)
XOR	Oracle	0.51 (0.02)	0.49 (0.01)	1.00 (0.00)	0.00 (0.00)	0.00 (0.00)	0.00 (0.00)	0.99 (0.00)
	Observed	0.80 (0.02)	0.52 (0.02)	1.00 (0.00)	0.35 (0.00)	0.07 (0.00)	0.00 (0.00)	0.61 (0.00)
	ICYM^{2}I	0.80 (0.02)	0.52 (0.02)	1.00 (0.00)	0.35 (0.00)	0.07 (0.00)	0.00 (0.00)	0.61 (0.00)

E SYNTHETIC DATA RESULTS

Data generation. Our work builds on the example introduced in (Liang et al., 2024a), in which we enforce additional missingness. Three latent variables (z_1, z_2, and z_c) are drawn from multi-dimensional clustered data; the observed covariates are a concatenation of z_c and one of the other latent variables, as illustrated in Figure 3. Then, the outcome Y is generated as $Y = \sigma(p_1\mathbb{E}(z_1) + p_2\mathbb{E}(z_2) + (1 - p_1 - p_2)\mathbb{E}(z_c))$, with the proportion $p_i \in [0, 1]$ such that $p_1 + p_2 \leq 1$. We simulate datasets with varying values of p_1 and p_2. Then, we enforce a 50% MAR missingness pattern in X_2 by modeling the probability of missingness. We do this by clustering X_1 into 100 groups using Kmeans. Then, the probability of missingness is generated using a random forest that regresses X_1 to predict $c_j \cdot Y$.

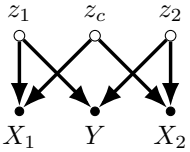

Figure 3. Data generating processes for synthetic experiments. z_i denote latent vectors, while all other variables are observed. Filled point nodes are observed variables, while unfilled nodes are unobserved.

Empirical setting. Data were split into three: 80% for training, 10% for validation, and the rest for testing. We consider neural networks with 2 hidden layers with 32 nodes, trained using an Adam optimizer (Kingma & Ba, 2014) with a learning rate of 0.001 over 100 epochs. Our evaluation relies on discriminative performance measured through AUROC.

Estimating predictive performance under Ω_{obs}. Table 9 presents the estimated performance obtained under different corrections. These results underline the importance of correcting both training and evaluation, as proposed in ICYM^{2}I, to best align with the performance one would obtain on Ω, as shown by the smallest Root Mean Squared Error (RMSE) observed when both corrections are applied. Note that in this setting, we rely on the true IPW correction that one would obtain with a properly specified model, as the MAR setting is met.

Table 9. Comparison between estimated AUC performance under the different training and evaluation corrections and oracle performance on Ω. ϵ denotes the RMSE between estimated and oracle PIDs.

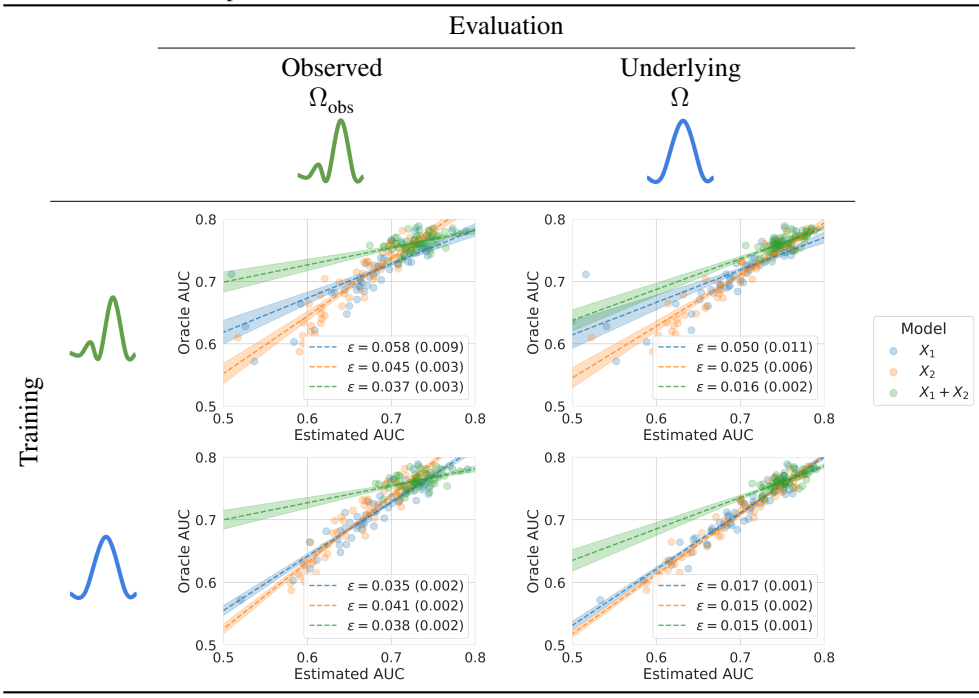

F SEMI-SYNTHETIC DATA RESULTS

F.1 UR-FUNNY

We illustrate the impact of missingness on estimating the informativeness of different modalities on real-world data with UR-FUNNY (Hasan et al., 2019), a multimodal dataset for humor detection from human speech used in affective computing. The dataset comprises text, audio, and visual modalities from 10 - 20 second videos sourced from TED talks, and the task is to detect whether a punchline would trigger a laugh. Labels were generated using the markup "(Laughter)" (Chen & Lee, 2017) from the transcript.

Dataset. The processed dataset from MultiBench (Liang et al., 2021) is a modality-complete dataset with 10,166 samples of paired audio, text, and vision embeddings. Audio embeddings were generated with COVAREP (Degottex et al., 2014), text with Glove (Pennington et al., 2014), and visual features through the Facet (Yuan et al., 2008) library and OpenFace (Baltrušaitis et al., 2016), and aligned using the Penn Phonetics Lab Forced Aligner (P2FA) (Yuan et al., 2008).

Enforcing missingness. To explore the impact of missingness on informativeness, we simulate a MAR missingness pattern on the audio and visual features given the textual modality. We vary the missingness from 30% to 70%, using the same mechanism as described for synthetic data. This semi-synthetic setting enables the evaluation of the proposed correction as the missingness mechanism is known. Note that the original dataset does not contain missing values, as the source data (TED Talks) have transcripts, and data labeling was generated based on these transcripts. However, settings with systematic transcripts are rare and may reflect a shift from the audio and textual modalities observed online for which such a match may not exist.

Results. Following the same empirical setting as in the synthetic experiment for each missingness rate, we measure the impact of missingness on PID decomposition. Figure 4 displays the PID values obtained under three strategies:

- Observed: All quantities are estimated using Ω_{obs}.
- ICYM^{2}I: All quantities are estimated using Ω_{obs} but corrected for the distribution shift through IPW.
- Oracle: All quantities are estimated on Ω.

This figure shows that the proposed strategy is consistently closer to the Oracle's PID values. This demonstrates that under Assumption C, the proposed correction yields better estimates of each modality's informativeness – specifically, the audio-visual modality (Unique 1) carries more information.

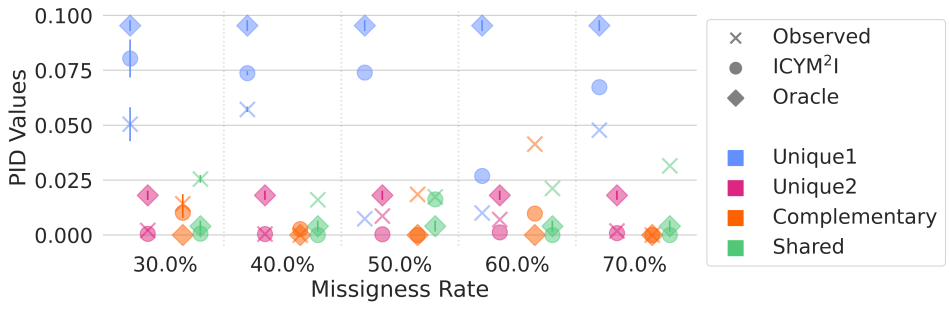

Figure 4: Comparison between estimated PID values under increasing missingness in UR-FUNNY.

F.2 HATEFUL MEMES

We run experiments using the dataset from the Hateful Memes Challenge (Kiela et al., 2020), which investigates text-image multimodal reasoning in the context of hate speech detection in online memes. The dataset comprises text-image pairs with an associated label indicating hate speech.

Dataset. We utilize the Kaggle version of the Facebook Hateful Memes dataset, as referenced in the Holistic Evaluation of Multimodal Foundation Models (HEMM) (Liang et al., 2024b) repository. Our analysis focuses on the 9,000 samples with associated labels. For each sample, embeddings were extracted for both modalities using a ResNet-50 (He et al., 2016) for images and a `BERT-base-uncased` (Devlin et al., 2019) model for text. The proposed ResNet-50 was pretrained on ImageNet (Deng et al., 2009) with the final layer replaced to extract 2048-dimensional feature vectors, and `BERT-base-uncased` (Devlin et al., 2019) extracts embeddings of dimension 784 from the penultimate layer.

Enforcing missingness. Similarly to the previous experiment, we vary the missingness from 30% to 70% by enforcing the same MAR missingness mechanism on the text modality, given the image modality, as we assume not all memes may contain text. Note that memes in the dataset were created by combining text from collected online memes with images sourced from stock images on Getty Images. Consequently, the dataset did not contain missing modality, but may not match the true distribution of memes one would observe online.

Results. As above, we measure the impact of increasing percentages of missingness on PID estimates. While the missingness mechanism results in a limited distribution shift, and therefore small differences in estimates between the corrected and observed strategies, the difference at 70% missingness shows the superiority of the proposed methodology in recovering the Unique contributions.

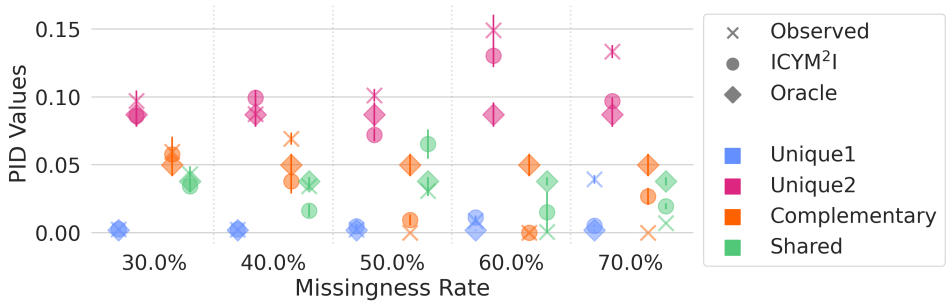

Figure 5. Comparison between estimated PID values under increasing missingness in Hateful Memes.

G STRUCTURAL HEART DISEASE DATA PROCESSING

All electrocardiograms were 10-second, standard 12-lead ECG signals collected at abstracted to 250 Hz, which we resampled to 500 Hz, and standard normalized by channel to match the inputs for ECG-FM (McKeen et al., 2024). We used the version of ECG-FM with weights pretrained on MIMIC-IV (Johnson et al., 2023; Goldberger et al., 2000) and PhysioNet 2021 (Reyna et al., 2021; 2022). We averaged the outputted feature embeddings along the temporal dimension and flattened them to produce vectors of length 768.

The chest radiographs used in our study were all postero-anterior (PA) view CXRs. We extracted pixel values from the DICOM files as grayscale images, center-cropped each image along the shorter dimension, applied contrast-limited adaptive histogram equalization (CLAHE) (Pizer et al., 1987) with a clip limit of 0.2, and resized each image to 1284×1284 pixels. All outputted embeddings were flattened to 4098-dimensional vectors.

H COMPUTE INFRASTRUCTURE

All experiments were performed on a server with an AMD EPYC 7313 CPU, 256 GB of memory, and two NVIDIA RTX A6000 GPUs, as well as a server with an Intel Xeon E5-2640 CPU, 128 GB of memory, and a NVIDIA GTX Titan X GPU. Our software stack includes Python 3.12, PyTorch 2.2.1 (Paszke et al., 2019), and standard Python scientific libraries. Chest radiograph embeddings used Tensorflow 2.19 (Abadi et al., 2015) and Tensorflow-Text 2.19 based on the requirements for the ELIXR models (Xu et al., 2023). Electrocardiogram embeddings were generated using an environment with Python 3.9 and fairseq-signals 1.0 to match the requirements for fairseq-signals and ECG-FM (McKeen et al., 2024). Generating embeddings for our structural heart disease data took approximately 10 hours on our server with a Titan X GPU. All synthetic experiments require 12 hours of compute time using one NVIDIA RTX A6000 GPU.